A Model of Baryons (Revised)

R Wayte

29 Audley Way, Ascot, Berkshire SL5 8EE, England, UK.

email: rwayte@googlemail.com

Abstract.

Baryons are considered to be intricate particles having real geometrical structure based on our earlier proton design. Inherent baryon spin is proportional to mass and radius. The well-known octets and decuplets fit into groups wherein mass-squared is associated with quantised-action. Magnetic moments are described in terms of a spin-loop and coupled electron(s). Lifetime of a baryon is governed by action of guidewave coherence around these structures.

Key words: baryon composite models
PACS Codes: 12.60.Rc, 14.20.Gk, 14.20.Jn, 13.30.Eg

1.   Introduction

Baryons are considered here to be complicated particles related directly to the earlier proton and meson designs [Wayte, Papers 1, 2]. Thus, half the mass energy consists of three trineons, bound together by their gluon field, travelling at the velocity of light around the spin-loop; at the centre of the spin-loop, there may also be a core particle which has zero net angular momentum. The remaining half mass energy consists of an external radial non-rotating pionic-type field, emitted by the trineons and core, plus electromagnetic field energy. Overall mass is entirely accounted for in terms of the localised energy constituting these parts; so there is no place for a Higgs ether theory.

For comparison, the Standard QCD model is a " black-box system" crafted to describe how particles interact with each other; but physical reality of the internal mechanism is secondary. Thus, quarks possess inherent charge and spin-½ even though they are formless singular points of infinite density; see Amsler et al (2008), Perkins (2000). The range in mass over the many particles of discrete mass is hardly addressed. There is also a problem with the origin of mass, entailing the ethereal Higgs field. Classical conservation laws are broken at will during various acts of materialisation. Fundamental problems like these have been reluctantly incorporated, in order to achieve some success at explaining empirical results by way of current quantum theory

In Section 2, the increase in particle angular momentum with mass-squared, for some baryons, is investigated to reveal an underlying action principle. The well known octets and decuplets are grouped here but other groups appear discordant. Section 3 covers strangeness and particle structure. Sections 4 and 5 explain magnetic moments and lifetimes in a way analogous to the proton and neutron. Section 6 shows how these models of internal structure can be compatible with aspects of QCD theory of particle interactions in order to explain observations. Baryon data has been taken from Patrignani C et al. (Particle Data Group), Chin. Phys. C, 40, 100001 (2016) and 2017 update.

2.   Spin relative to mass-squared for some baryons

2.1   J versus M^2.   Several Δ and Λ baryons appear to have spin angular momentum (J) proportional to their mass-squared (M^2), as demonstrated in a Chew-Frautschi plot. This is thought to result from a particular internal mechanism. Figure 2.1 illustrates the cases in which two or more baryons of a given species lie on straight parallel lines which obey the expression:

$$M^2 \approx 2(J+A) \times (37.7^2 m_e)^2 \, , \tag{2.1}$$

where $(37.7 \approx 12\pi)$ relates to a structure constant from Paper 1, and m_e is the electron mass. For *these selected* baryons only, factor (A) will be taken to represent the proportion of mass which does not contribute to the spin. Its value appears to be a multiple of (1/6), so let [(J+A) = N/6] for an integral N; then Eq.(2.1) simplifies to:

$$M^2 \approx (N/3)(37.7^2 m_e)^2 \quad . \tag{2.2a}$$

This expression may take other numerical forms, for later consideration:

$$M^2 \approx 3N \times [137 \times 3 \, (\pi/e_n) \times m_e]^2 \approx N(6 \times 137 \times m_e)^2 , \tag{2.2b}$$

where $(137 \approx \hbar c/e^2)$ is the inverse fine structure constant, and $(e_n = 2.71828)$. Factor (π/e_n) has previously signified gluon involvement, so coefficient 3 may pertain to trineon pearls with their gluonic field.
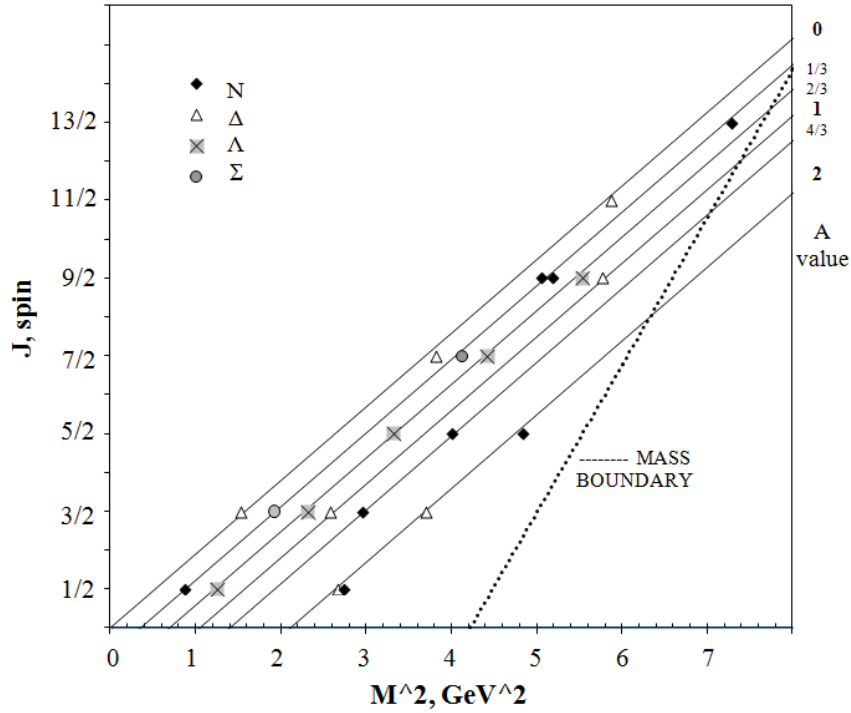

Figure 2.1   Selected baryons which lie on straight parallel lines obeying Eq.(2.1) for the various values of A given. The theoretical *mass boundary* line is derived later as Eq.(2.8).

To interpret these expressions in terms of baryon structure, we will let J represent real spin angular momentum due to mass M_1 in a spin-loop, while A represents a spin-less mass M_2 at the baryon centre. Many mesons analysed in Paper 2 have this two part configuration; consequently, we will propose an *action* expression for the simplest design:

$$\left(\frac{M_1}{2}\right)cR2\pi + \left(\frac{M_2}{2}\right)c^2\tau = (J+A)h \quad , \tag{2.3a}$$

where spin radius R will later be set proportional to total mass $(R = F_b M/c^2)$, and the spin period is $(\tau = 2\pi R/c)$. Then the first term is momentum-action over one orbit, and the second term is the associated energy-action of the core mass. As found for the proton, only half the mass $(M_1/2, M_2/2)$ is involved in this expression because the other half mass is in the exterior field. Now, $(M = M_1 + M_2)$, therefore:

$$\frac{M}{2}cR2\pi = (J+A)h = 2\pi\left(\frac{F_b}{c}\right)\frac{M^2}{2} \quad , \tag{2.3b}$$

and using Eq.(2.1), the constant F_b can take a universal form:

$$F_b \approx \frac{137}{37.7^4}\left(\frac{e}{m_e}\right)^2 \approx 6\times37.7\left(\frac{e}{m_p}\right)^2 \quad , \tag{2.3c}$$

where m_p is the proton mass. For this simplest case, the spin-mass and core-mass are given by:

$$M_1 = M\left(\frac{J}{N/6}\right), \quad M_2 = M\left(\frac{A}{N/6}\right) \quad , \tag{2.4}$$

and these do not appear to take any special noteworthy values for the Λ baryons in Figure 2.1. Coefficient N does not represent the number of component pieces constituting M. The three Δ baryons shown with $(A = 0)$ have no core particles.

Equation (2.3a) expresses the fermion spin radius R for the spinning mass M_1 , when R is proportional to total mass M:

$$R = \frac{2J\hbar}{M_1c} = \frac{2(J+A)\hbar}{Mc} = \frac{F_bM}{c^2} \quad , \tag{2.5a}$$

and for stability there is an integral number of Compton guidewavelengths around the spin-loop:

$$2\pi R = 2J(h/M_1c) \quad . \tag{2.5b}$$

Empirically, we shall see in Section 3 that this simplest case does not apply to most baryons because the spin-loop probably consists of 9 proton-pearls for stability, and the core mass is comparatively small. This necessitates Eq.(2.4) to be developed, namely:

$$M_1 = M\left(\frac{J+\varepsilon}{N/6}\right), \quad M_2 = M\left(\frac{A-\varepsilon}{N/6}\right) \quad , \tag{2.6a}$$

where (ε) is a multiple of $(1/6)$ like J and A, selected for each baryon. Then, Eq.(2.3a) should be written:

$$\left(\frac{M_1}{2}\right)cR2\pi + \left(\frac{M_2}{2}\right)c^2\tau = [(J+\varepsilon)+(A-\varepsilon)]h \quad . \tag{2.6b}$$

2.2   A versus J.   Figure 2.2 shows plots of A versus J for baryons in five species. It appears that A accommodates the prevailing J almost arbitrarily, as if most baryons are not designed to obey Eqs.(2.1), (2.3a). The aggregate plot on the right shows how some A values are occupied up to 4 times, while others are vacant. For example, when $(J = \frac{1}{2})$, values of

($A \times 6$ = 1, 3, 6, 11) are absent but others are present up to 18. It will be shown in the next section that some values of N are preferred, governed by internal action.

The empirical diagonal boundary line in Figure 2.2 describes A through the form:

$$A_b = -\frac{3}{6}J + \frac{24}{6} \quad . \tag{2.7a}$$

It cuts the abscissa at ($2J_{max}$ = 16, A = 0) where the maximum theoretical mass through Eq.(2.1) is:
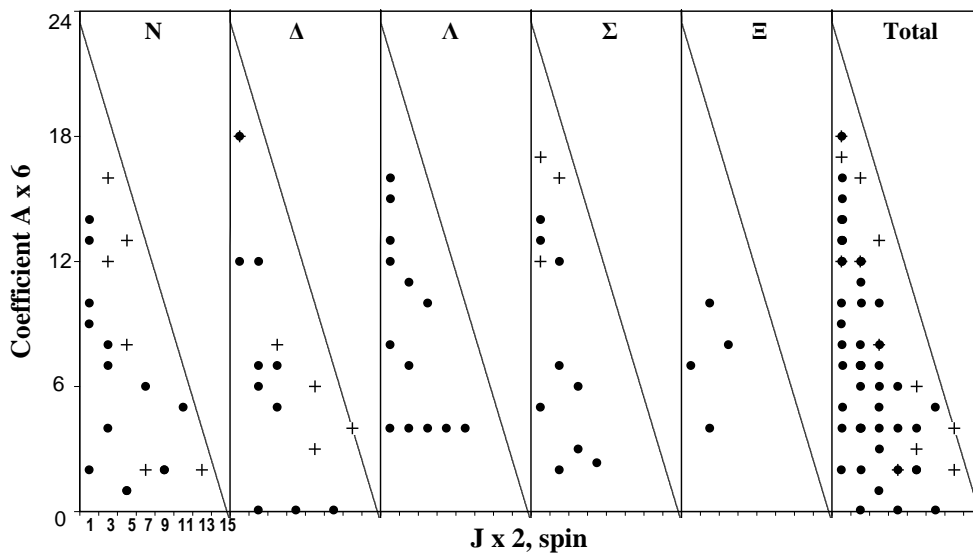
$$M_{max} = 2905 \text{MeV}/c^2 . \tag{2.7b}$$

Figure 2.2   Plots to show how factor A varies with spin J for each type of baryon. The points lie within a common boundary line, and the Λs and Ξs may have a zone of avoidance at low A values. Baryons of 2-star quality have also been included (+).

At the other end (J = 0, $A_{max} \approx 24/6$), the mass is only:

$$M = M_{max}/\sqrt{2} \quad , \tag{2.7c}$$

so ($A_{max} = J_{max}/2$). Upon introducing Eq.(2.7a) into Eq.(2.1), an empirical mass boundary may be drawn on Figure 2.1 as shown for:

$$M_b{}^2 \approx 2 \times \left(\frac{3}{6}J + \frac{24}{6}\right)(37.7^2 m_e)^2 . \tag{2.8}$$

Thus, hypothetically, a baryon of (J = 15/2) and maximum mass 2859MeV/c^2 could contain 3 trineons of proton mass.

2.3 **Quantisation of N.** Baryon mass-squared given by N (nearest) in Eq.(2.2a) may be plotted to reveal quantisation patterns, (data from PDG Baryon Tables). Figure 2.3a shows confirmed baryons up to Ω^-, and many of them linked by an increment ($\delta N = 6$) have been emphasised as the Os and Xs. Several other intervals of ($\delta N = 3$) are apparent. Figure 2.3b illustrates groups of the same spin-parity, including the well-known baryon octet $(1/2)^+$, decuplet $(3/2)^+$, groups $(5/2)^+$ and $(7/2)^+$. For each group, factor N increases through the species range $\mathcal{N}$, $\boldsymbol{\Delta}$, $\boldsymbol{\Lambda}$, $\boldsymbol{\Sigma}$, $\boldsymbol{\Xi}$, $\boldsymbol{\Omega}$ so factor A must be increasing even if interpretation Eq.(2.3a) may not apply.

Significant characteristics of Figure 2.3a are:

1. Five of the $\boldsymbol{\Lambda}$s increase in equal steps of ($\delta N = 6$) from (N = 7 to 31), while their spin-parity increases as $(1/2^+, 3/2^-, 5/2^+, 7/2^-, 9/2^+)$, and (A = 4/6) is constant.

2. Four of the $\boldsymbol{\Sigma}$s increase in equal steps of ($\delta N = 6$) from (N = 11 to 29), with their spin-parity increasing as $(3/2^+, 5/2^-, 7/2^+, 9/2^-)$, and (A = 2/6) is constant.

3. Five of the $\boldsymbol{\Xi}$s increase in equal steps of ($\delta N = 3$), from (N = 10 to 22) with their spin-parity varying as $(1/2^+, 3/2^+, 1/2^-?\ 3/2^-, 1/2^+?\ )$, and A varying as (7/6, 4/6, 13/6, 10/6, 19/6). The queried values need confirmation.

4. Three of the $\boldsymbol{\Delta}$s increase in equal steps of ($\delta N = 12$) as (N = 9, 21, 33), while their spin-parity increases as $(3/2^+, 7/2^+, 11/2^+)$, and (A = 0) is constant.

5. Three of the $\mathcal{N}$s increase in equal steps of ($\delta N = 12$) as (N = 5, 17, 29), while their spin-parity increases as $(1/2^+, 3/2^+, 9/2^-)$ and A varies.

6. Three other $\mathcal{N}$s increase in equal steps of ($\delta N = 6$) as (N = 15, 21, 27), with their spin-parity increasing as $(1/2^-, 3/2^+, 7/2^-)$ and A varying.

7. A wide range of $\boldsymbol{\Lambda}$ masses with (N = 7, 11, 15, 16, 18, 19) have spin-1/2.

8. Those massive $\mathcal{N}$s with (N = 27, 28, 29, 38) have high spin values (7/2, 9/2, 9/2, 11/2).

9. Massive baryons in general have greater spin with larger circumferences, as if to reduce material density. Therefore, maximum density may exist for [$\boldsymbol{\Delta}$(1910) ½+] or [$\boldsymbol{\Xi}$(1950) ½+].
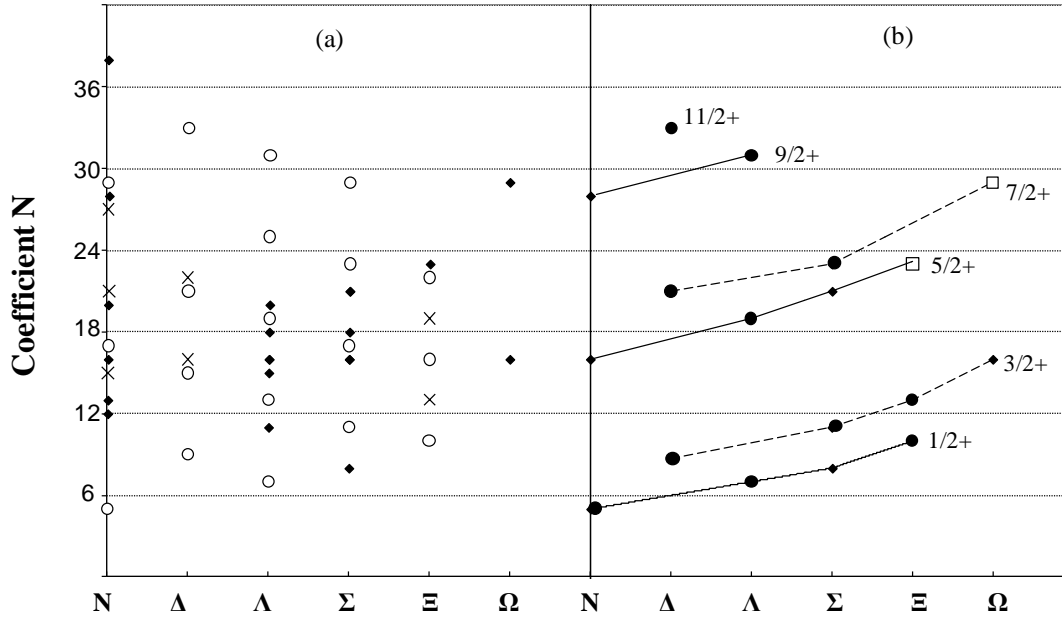
Figure 2.3   (a) Quantisation number N plotted to reveal patterns for the six species of baryons. The Os and Xs are the noteworthy points of a pattern linked by ($\delta N = 6$, or 12).

(b) The grouping of baryons with the same spin-parity into octet, decuplet and smaller groups reveals partial correspondence with the noteworthy points in part (a), see 11 larger spots. Baryons shown as □ need confirmation.

The most occupied value of N in Figure 2.3a is 16, where for example (J = 3/2, A = 7/6) or (J = 5/2, A = 1/6). Then Eq.(2.2a) evaluates to:

$$M \approx 1677 \text{MeV} / c^2 = 4\sqrt{N} m_x$$

$$\text{for} \quad m_x = \frac{37.7^2}{4\sqrt{3}} m_e = 104.8 \text{MeV} / c^2 , \tag{2.9}$$

which is near to the proton-pearl mass ($m_\ell = m_p/9 = 104.25 \text{MeV}/c^2$). However, this does not necessarily mean that there are 16 pearls in these baryons, because N is concerned with units of *action*, see Eq.(2.10). For our proton model, N is 5 but there are 9 pearls.

Except for the Λs and Δs on the lines in Figure 2.1, it is impossible to know whether N should be split into J and A components. Again, the proton has (N = 5) which might imply that (A = 2/6) for a particle core, but this would be wrong. Consequently, the N value may not be interpretable as 6(J + A) because for example, the material may all be in the spin-loop at a radius which decreases with mass but increases with J as in Eq.(2.6a) when ($M_1 \rightarrow M$).

In Figure 2.3a, the way that N clearly increments most often by a multiple of ($\delta N = 6$) will be explained by introducing it into Eq.(2.3b) to produce a precise *action increment (h)* for many baryons:

$$\left(\frac{\delta N}{6}\right)h = h \approx \delta\left(\frac{M}{2}c2\pi R\right) \quad ; \tag{2.10a}$$

or for mass-squared, Eq.(2.2a) gives:

$$\delta\left(M^2\right)_6 \approx 2\times(37.7^2\, m_e)^2 \quad . \tag{2.10b}$$

Therefore, the members of a species often increase in steps of mass-squared by *adding* action (h) quanta. If A is held constant say, then J must increase by unity (e.g. from $^1/_2$ to $^3/_2$). Since the different species clearly show ($\delta N = 6$), they probably have a common structure. Smaller action increments also occur; for example ($\delta N = 1$), then Eq.(2.2a) produces:

$$\delta\left(M^2\right)_1 \approx \left(\frac{37.7^2}{\sqrt{3}}\, m_e\right)^2 \approx \left(6\times 137 m_e\right)^2 \quad . \tag{2.10c}$$

Given that the nucleon-nucleon force constant is ($1/\sqrt{3}$) in Paper 1, this expression contains three fundamental constants. For the most occupied value of ($N = 16$), this Eq.(2.10c) means that:

$$\left(M^2\right)_{16} \approx \left(24\times 137 m_e\right)^2 \quad , \tag{2.10d}$$

which reflects another structure constant seen in Paper 1, (24 loops in a proton pearl). According to Eq.(2.9), an increment in N from 16 to 17 requires an increase in mass of $m_x/2$.

It is possible that *all* baryon masses are stable configurations determined primarily by an *action principle* related to absolute M^2 because there are examples of N incrementing by 6, 4, 3, 2 or 1, in addition to those satisfying Eq.(2.3a,b). Then according to Eq.(2.2a), total action of a baryon's existence for one spin-loop period is equal to:

$$\left(\frac{N}{6}\right)h \approx \left(\frac{1}{2\times 37.7^4}\right)\left(\frac{M}{m_e}\right)^2 h \quad . \tag{2.10e}$$

This expression applies whatever the mass M_1 happens to be in the spin-loop, and spin radius is given by:

$$R = 2J\frac{\hbar}{M_1 c} \quad . \tag{2.10f}$$

These two independent conditions can be combined by introducing a coefficient (n) into Eq.(2.3a) to compensate for small J and A values, while N may be large:

$$n\left(\frac{M_1}{2}\right)cR\,2\pi + n\left(\frac{M_2}{2}\right)c^2\tau = n(J+A)h = \frac{N}{6}h \ . \tag{2.10g}$$

For example, the proton has no core particle so (J = 1/2, A = 0, n = 5/3, N = 5). In effect, (n) becomes equivalent to a number of spin-loop periods. High mass baryons with small spin can be accommodated this way. A baryon like $\Delta(1600)$ which would appear to fit well on the (A = 0) line at (J = 5/2) in Figure 2.1 has instead fitted (J = 3/2, A = 1). Thus, given a measured M and J for any baryon, interpretation Eq.(2.10g) may apply more often than Eq.(2.3a,b).

In Figure 2.3b, the groups $J^P = 1/2^+$, $J^P = 5/2^+$ and $J^P = 9/2^+$, for ($\mathscr{N}$, Λ, Σ, Ξ) appear to be related approximately. Likewise, groups $J^P = 3/2^+$, $J^P = 7/2^+$ and $J^P = 11/2^+$, for (Δ, Σ, Ξ, Ω) appear related. The absolute (mass)^2 difference between these groups for ($\delta N \approx 12$) in Eq.(2.2a) may be expressed as:

$$(M_5{}^2 - M_1{}^2) \approx (M_9{}^2 - M_5{}^2) \approx (M_7{}^2 - M_3{}^2) \approx 4\times(37.7^2 m_e)^2 . \tag{2.11}$$

This is a square-law relationship, so the mass of any M_5 baryon relative to its M_1 baryon depends upon its species. They probably have similar designs and primarily satisfy *action* expressions like Eq.(2.10a,b). The same could be said for (M_9) relative to (M_5), and (M_7) relative to (M_3) groups. When J changes by 2 between these groups, then individual A values change little or not at all.

The low positioning of the decuplet $3/2^+$ group between the octet $1/2^+$ and $5/2^+$ groups implies that each member is deficient by ($\delta N \approx 3$) due to a reduced A value. The same could be said for the low positioning of the $7/2^+$ group.

Figure 2.4b shows the second ($J^P = 1/2^+$) group as having N values greater than the lowest octet by ($\delta N \approx 7\text{-}8$). The third ($J^P = 1/2^+$) group runs parallel to the lowest octet at ($\delta N \approx 12$), so *action* equation (2.10a) is clearly operating. Possibly, Eq.(2.3a) would imply a large spin-less central mass M_2; on the other hand, these heavier groups with small J might be compact, obeying Eq.(2.10g) with small mass M_2 but large (n).
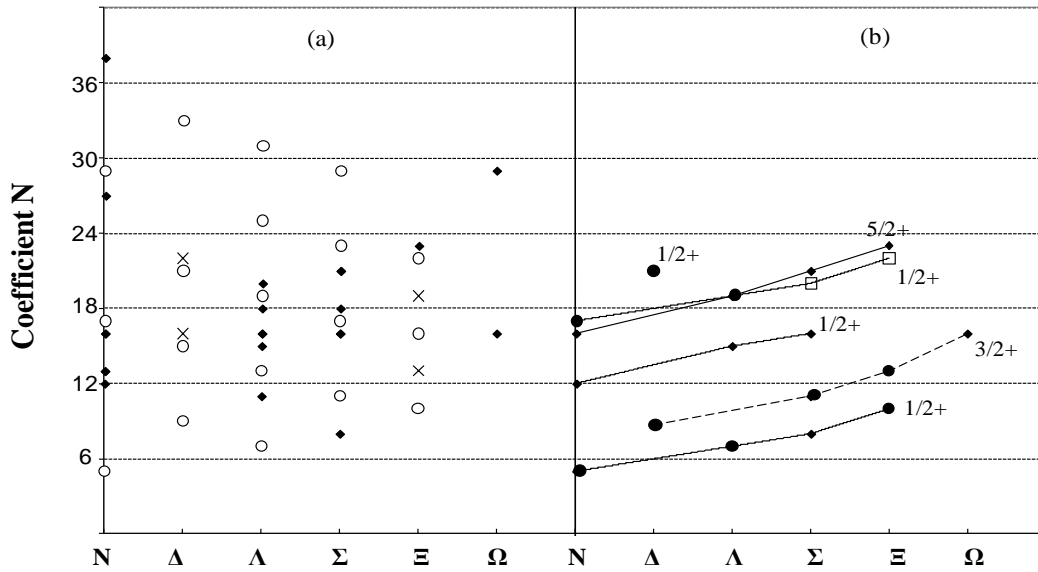
Figure 2.4   (a) Quantisation number N plotted for the six species of baryon.
(b) The higher mass ($J^P = 1/2^+$) groups are shown relative to standard ($J^P = 5/2^+$, $3/2^+$, $1/2^+$) groups.

Figure 2.5b shows the ($J^P = 1/2^-$) groups as having extra mass, with ($\delta N \approx 7\text{-}11$) relative to the lower ($J^P = 1/2^+$) octet. Again, these baryons must be physically small, to contain the mass without increasing spin, or they have large central masses.
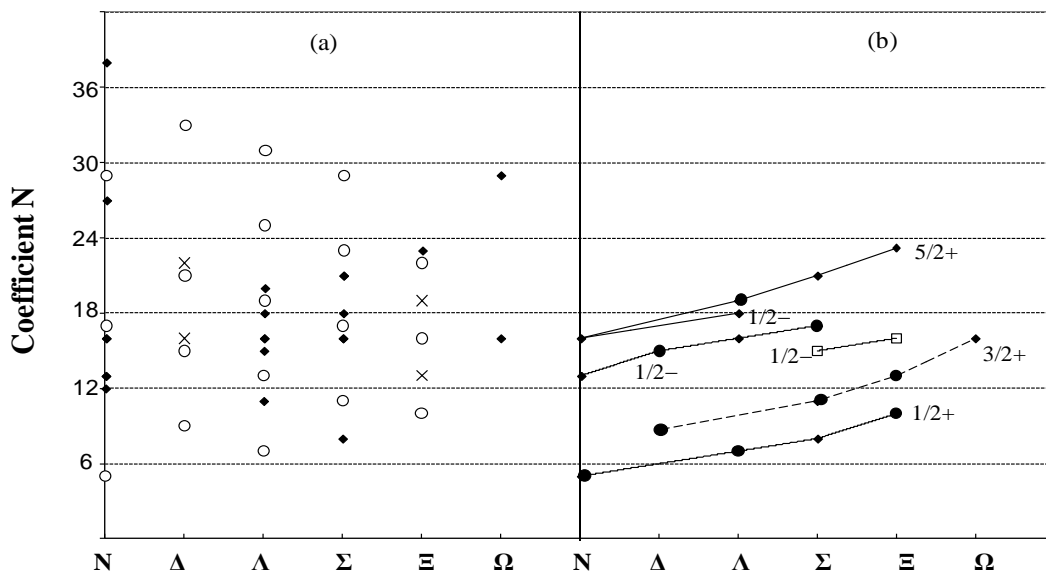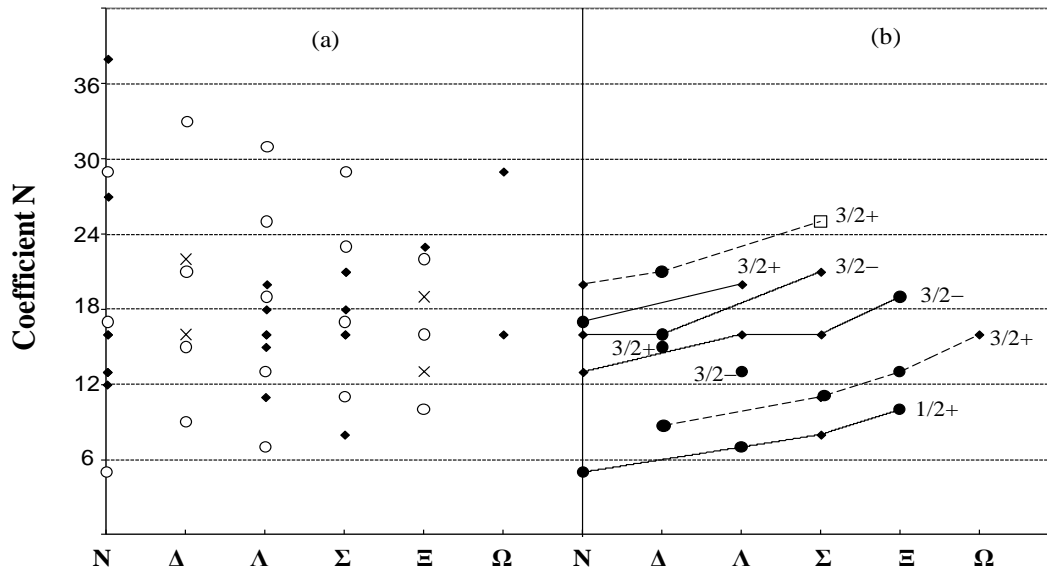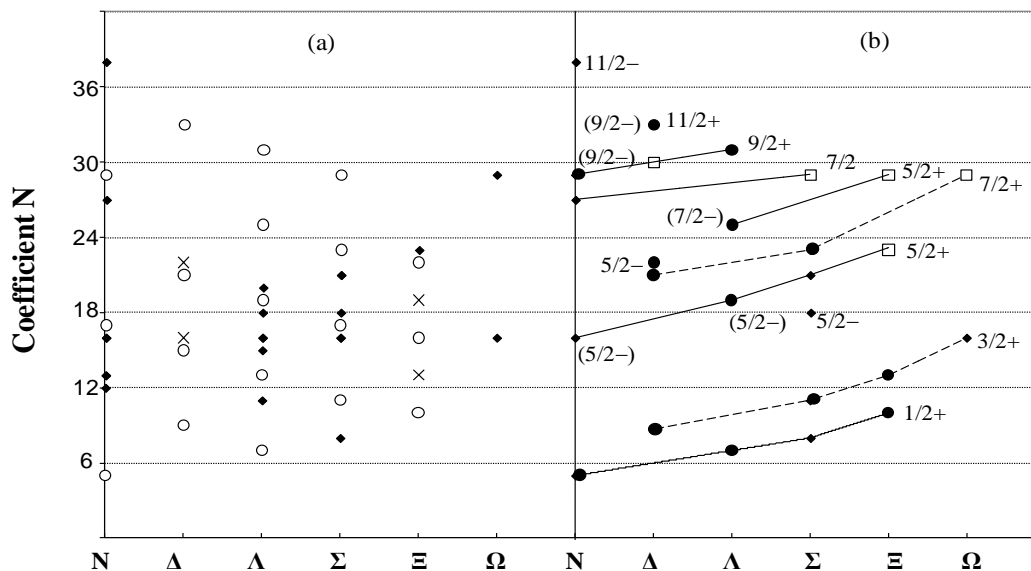

Figure 2.5   (a) Quantisation number N plotted for the six species of baryon.
(b) The higher mass ($J^P = 1/2^-$) groups are shown relative to the standard ($J^P = 5/2^+$, $3/2^+$, $1/2^+$) groups.

Figure 2.6b shows the ($J^P = 3/2^-$) group as having increased N values; eg., ($\delta N \approx 6$) relative to the lower original ($J^P = 3/2^+$) decuplet. Two higher mass ($J^P = 3/2^+$) groups are also shown.

Figure 2.6   (a) Quantisation number N plotted for the six species of baryon.

(b) Two higher mass ($J^P = 3/2^-$) groups are shown relative to the standard ($J^P = 3/2^+$, $1/2^+$) groups.

Figure 2.7b shows the higher mass ($J^P = 5/2^+$) group as having N values greater than the lower ($J^P = 5/2^+$) octet by ($\delta N \approx 6$).

Figure 2.7   (a) Quantisation number N plotted for the six species of baryon.

(b) The higher mass ($J^P = 5/2^+$) group and various weakly-grouped species are shown relative to the standard ($J^P = 5/2^+$, $3/2^+$, $1/2^+$) groups. Terms in brackets represent additional baryons with different J^P values but similar mass.
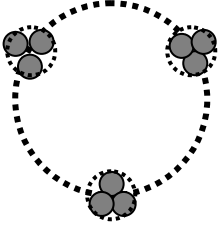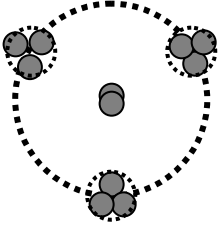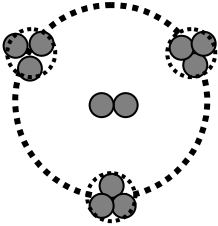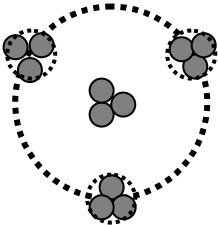
3.   Strange, charmed and bottom baryons

The concept of baryon strangeness is founded upon the very long lifetimes of those with the lowest mass in their group, $\Lambda(1116)$, $\Sigma(1193)$, $\Xi(1315)$, $\Omega^-(1672)$. More massive strange baryons have short lifetimes, so strangeness is only apparent upon decay into their lowest states. Accordingly, strange baryons appear to possess a latent structure which is transferred during rapid decay, until at the lowest level it is revealed by a relatively long lifetime. The following proposed designs assume that baryons are an assembly of parts so that decay is a disintegration process, with minimal creation of any new particles and kinetic energy. The observed repeatability of creation and decay processes, and baryon masses, requires distinct components of discrete sizes; otherwise a continuum of masses and species would exist.

There appears to be a need to satisfy Eq.(2.10) with N increasing in possible steps of ($\delta N = 6, 3, 2, 1$), but at the same time M probably consists of a number of well-defined stable pieces which separate during decay processes. These two conditions can be satisfied only approximately by building baryons from proton-pearl masses (m_ℓ) for the spin loop, and pionet masses for the core (ie. a miniaturised pion, $m_{\pi o} = 134.976 \text{MeV/c}^2$, and ($m_{\pi o}/4 = 33.744 \text{MeV/c}^2$) which is the mass of a pionic pearl, in Paper 2). The many cases of baryons of one species decaying into other species and back indicate that they are all similar in essence, using a range of common component parts combined in various ways with correspondingly different binding energies. Equation (2.6a) is used to calculate individual values for (ε) after setting $M_1 = m_p$.

Table 1a illustrates feasible designs for ($J^P = 1/2^+$) baryons, with their N (nearest) values plus corresponding masses. The proton has 3 trineons consisting of 3 pearls each, (Paper 1).
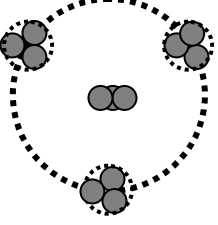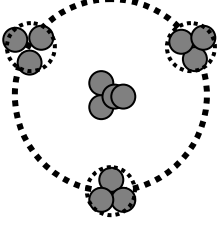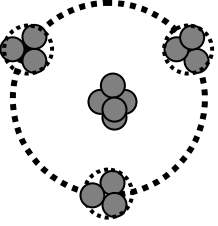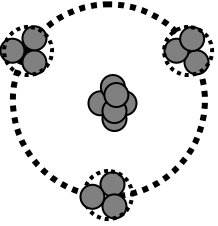
Table 1a. Proposed structure for the ($J^P = 1/2^+$) baryon octet.

p		**p(938)** $\frac{1}{2}(\frac{1}{2}^+)$ $m_p \approx 938.272\,\mathrm{MeV}/c^2$ $N = 5, \quad A = 1/3, \quad \varepsilon = 1/3$
Λ		**Λ(1116)** $0(\frac{1}{2}^+), \tau = 2.632 \times 10^{-10}\mathrm{s}, Dy(p\pi^-, n\pi^o)$ $m \approx m_p + 1\frac{1}{2}\,m_{\pi o} \approx 1141\,\mathrm{MeV}/c^2,$ $N = 7, \quad A = 2/3, \quad \varepsilon = 1/2$
Σ		**Σ(1190)** $1(\frac{1}{2}^+), \tau = 0.8018 \times 10^{-10}\mathrm{s},$ $Dy(p\pi^o, n\pi^+, \Lambda\gamma)$ $m \approx m_p + 2m_{\pi o} \approx 1208\,\mathrm{MeV}/c^2,$ $N = 8, \quad A = 5/6, \quad \varepsilon = 1/2$
Ξ		**Ξ^0(1315)** $\frac{1}{2}(\frac{1}{2}^+), \tau = 2.90 \times 10^{-10}\mathrm{s}, Dy(\Lambda\pi^o)$ $m \approx m_p + 3m_{\pi o} \approx 1343\,\mathrm{MeV}/c^2,$ $N = 10, \quad A = 7/6, \quad \varepsilon = 2/3$

In Table 1b, the ($J^P = 3/2^+$) baryon decuplet reveals strangeness operating without apparently satisfying Eqs.(2.3a,b). Non-strange baryon Δ(1232) consists of a spin-loop, comprising 3 trineons of 3 proton-pearls each, plus a central core of $2\frac{1}{4}$ pionets. If a Δ(1232) were to consist of only a spin-loop comprising 3 trineons of 4 proton-pearls each, then the decay process into $N\pi$ would be less straightforward because a pion consists of 50% antimatter. Strange Σ(1385) has a spin-loop of 9 proton-pearls plus a central $3\frac{1}{2}$ pionets. The Ξ(1530) has 4½ core pionets, and the Ω^-(1672) has 5½ core pionets, 4 of which become a
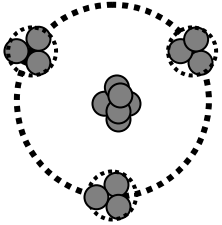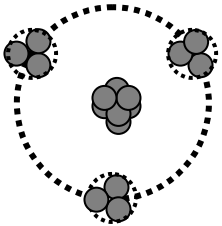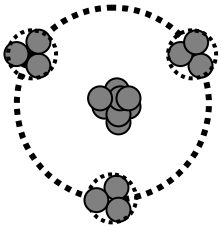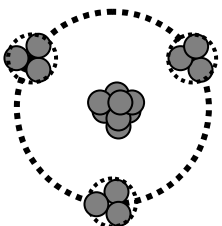
K⁻ during decay. Numerical exactness between theoretical and experimental masses is not expected because unspecified binding energy will depend upon the particular designs.

Table 1b. Proposed structure for the ($J^P = 3/2^+$) baryon decuplet.

Δ		**Δ(1232)** $^3/_2(^3/_2{}^+)$, $\Gamma = 118$ MeV, Dy(Nπ) $m \approx m_p + 2\tfrac{1}{4}m_{\pi o} \approx 1242\,\text{MeV}/c^2$, $N = 9$, $A = 0$, $\varepsilon = -1/3$
Σ		**Σ(1385)** $1(^3/_2{}^+)$, $\Gamma = 36$ MeV, Dy($\Lambda\pi,\Sigma\pi,\Lambda\gamma$) $m \approx m_p + 3\tfrac{1}{2}m_{\pi o} \approx 1410\,\text{MeV}/c^2$ $N = 11$, $A = 1/3$, $\varepsilon = -3/12$
Ξ		**Ξ(1530)** $^1/_2(^3/_2{}^+)$, $\Gamma = 9.1$ MeV, Dy($\Xi\pi$) $m \approx m_p + 4\tfrac{1}{2}m_{\pi o} \approx 1545\,\text{MeV}/c^2$ $N = 13$, $A = 2/3$, $\varepsilon = -1/6$
Ω⁻		**Ω⁻(1672)** $0(^3/_2{}^+)$, $\tau = 0.821 \times 10^{-10}$s, Dy($\Lambda$K⁻,$\Xi\pi$) $m \approx m_p + 5\tfrac{1}{2}m_{\pi o} \approx 1681\,\text{MeV}/c^2$ $N = 16$, $A = 7/6$, $\varepsilon = 0$

In Table 1c, the ($J^P = 5/2^+$) baryon group reveals strangeness operating without satisfying Eqs.(2.3a,b). Non-strange baryon $\mathcal{N}$(1680) consists of a spin-loop, comprising 3 trineons of 3 proton-pearls each, plus 5½ core pionets. Strange Λ(1820) has a similar spin-loop but 6½ core pionets, 4 of which become a $\overline{K}$ during the decay process. The Σ(1915) has 7½ core pionets, and the Ξ(2030) has 8.

Table 1c. Proposed structure for the ($J^P = 5/2^+$) baryon group.

$\mathcal{N}$		**$\mathcal{N}$ (1680)** $^{1}/_{2}(^{5}/_{2}{}^{+})$, Γ =130 MeV, Dy(Nπ) $m \approx m_p + 5\frac{1}{2}m_{\pi o} \approx 1681\,\text{MeV}/\text{c}^2$ $N = 16$, $A = 1/6$, $\varepsilon = -1$
Λ		**Λ(1820)** $0(^{5}/_{2}{}^{+})$, Γ =80 MeV, Dy(N$\overline{K}$, $\Sigma\pi$) $m \approx m_p + 6\frac{1}{2}m_{\pi o} \approx 1816\,\text{MeV}/\text{c}^2$ $N = 19$, $A = 2/3$, $\varepsilon = -11/12$
Σ		**Σ(1915)** $1(^{5}/_{2}{}^{+})$, Γ =120 MeV, Dy(N$\overline{K}$) $m \approx m_p + 7\frac{1}{2}m_{\pi o} \approx 1951\,\text{MeV}/\text{c}^2$ $N = 21$, $A = 1$, $\varepsilon = -5/6$
Ξ		**Ξ(2030)** $^{1}/_{2}(^{5}/_{2}{}^{+})$, Γ =20 MeV, Dy($\Lambda\overline{K}$, $\Sigma\overline{K}$) $m \approx m_p + 8m_{\pi o} \approx 2018\,\text{MeV}/\text{c}^2$ $N = 23$, $A = 4/3$, $\varepsilon = -2/3$

Other groups (J^P = $7/2^+$, $1/2^-$, $3/2^-$, etc) are probably based upon these structures because Figure 2.3 is linked to Eqs.(2.10) and (2.11), in regard to *action* requirements.

In these three tables above we have used the proton spin-loop mass for all, while varying the core mass. However, the six types of baryon must have different designs, as indicated by the observed magnetic moments given in Table 4. For example, in the proton design of Paper 1, the 3 trineons and 9 pearls rotate anti-parallel to the spin-loop, thereby opposing the spin-loop's magnetic moment. In Table 1d we set these trineons, pearls and the

core particle to rotate parallel or anti-parallel to the spin-loop, in order to account for the six types of baryon. These orientations will affect the interactions and binding energy/mass of each baryon. All six species have a baryon in the $N = 16$, $M \approx 1677 \text{MeV/c}^2$ range. Decay from one species to another will be fast or slow, subject to conservation of spin and whether the spin has to change orientation or not.

Table 1d. The proposed orientations of trineons, pearls, and core particle for six species of baryons.

	$\mathcal{N}$	Δ	Λ	Σ	Ξ	Ω
Spin of all 3 trineons	anti-parallel	anti-parallel	parallel	parallel	parallel	parallel
Spin of all 9 pearls	anti-parallel	anti-parallel	anti-parallel	anti-parallel	parallel	parallel
Net core spin	anti-parallel	parallel	parallel	anti-parallel	anti-parallel	parallel

Charmed baryons. In Tables 2a,b the proposed structures for some charmed baryons of spin $1/2^+$ and $3/2^+$ are given. These have a spin-loop of mass $2m_p$ and a central core of muonets with overall zero spin. A muonet has mass ($m_\mu' = (^4/_3)m_\mu = 140.88 \text{MeV/c}^2$), as commonly used for mesons in Paper 2. Each trineon here has the mass of two proton-trineons and it is expected to have a radius of $(\pi/2)(e^2/2m_pc^2)$, which is $137(2/\pi)$ times less than the baryon spin-loop radius. This trineon mass consists of matter plus anti-matter given that $\Lambda_c(2880)^+$ and $\Lambda_c(2940)^+$ can decay into a proton plus a $D^0(1864.84)$ meson made of 50% anti-matter. The mass range of charmed baryons appears limited, from $(2m_p + 3m_\mu')$ for Λ_c^+ (2286.46) to $(2m_p + 8.5m_\mu')$ for $\Xi_c(3080)$. Where appropriate, the mass difference between charged components of a baryon is given. For example, for Σ_c (2455), the mass difference $(m^0 - m^+)$ is due to a single heavy-electron orbiting around the positive spin-loop, while $(m^{++} - m^+)$ is due to an orbiting heavy-positron. These heavy electron or positron will help determine any magnetic moments, as explained in Section 4.

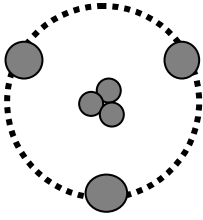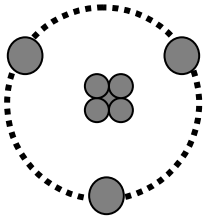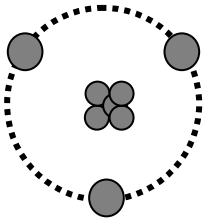Table 2a.   Proposed structure for the charmed baryons with ($J^P = 1/2^+$).
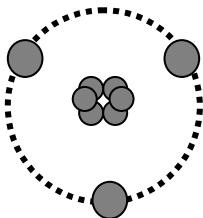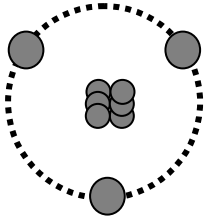
Λ_c^+	**Λ_c^+ (2286.46)** $0(^1/_2{}^+)$, $\tau = 200 \times 10^{-15}$s, Dy($pK^-\pi^+$) $m \approx 2m_p + 3m'_\mu \approx 2299\,\text{MeV}/c^2$ $N = 30$, $A = 9/2$, $\varepsilon = 11/3$
Σ_c	**Σ_c (2455), $m^{++}-m^+= 2.1 m_e$, $m^0-m^+=1.66 m_e$** $1(^1/_2{}^+)$, Dy($\Lambda_c^+ \pi$) $m \approx 2m_p + 4\frac{1}{4}m'_\mu \approx 2475\,\text{MeV}/c^2$ $N = 34$, $A = 31/6$, $\varepsilon = 23/6$
Ξ_c^+	**Ξ_c^+(2467.87), $m^0-m^+ = 5.87 m_e$** $^1/_2(^1/_2{}^+)$, $\tau = 442 \times 10^{-15}$s, Dy($\Xi^-2\pi^+$) $m \approx 2m_p + 4\frac{1}{4}m'_\mu \approx 2475\,\text{MeV}/c^2$ $N = 35$, $A = 16/3$, $\varepsilon = 4$
Ω_c	**Ω_c^o(2695.2)** $0(^1/_2{}^+)$, $\tau = 69 \times 10^{-15}$s, Dy($\Sigma^+K^-K^-\pi^+$) $m \approx 2m_p + 6m'_\mu \approx 2722\,\text{MeV}/c^2$ $N = 41$, $A = 19/3$, $\varepsilon = 25/6$

Table 2b.   Proposed structure for the charmed baryons with ($J^P = 3/2^+$), plus the most massive confirmed charmed baryon.
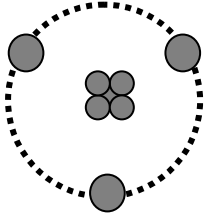
Σ_c	**Σ_c (2520),** **($m^{++}- m^+ = 1.78m_e$; $m^0 - m^+ = 1.92m_e$)** $1(^3/_2{}^+)$, $Dy(\Lambda_c{}^+ \pi)$ $m \approx 2m_p + 4\tfrac{1}{2}\, m'_\mu \approx 2511\,\mathrm{MeV/c^2}$ $N = 36,\quad A = 9/2,\quad \varepsilon = 3$
Ξ_c	**Ξ_c(2645), ($m^0 - m^+ = 1.54m_e$)** $^1/_2(^3/_2{}^+)$, $Dy(\Xi_c{}^0\pi^+, \Xi_c{}^+\pi^-)$ $m \approx 2m_p + 5\tfrac{1}{2}\, m'_\mu \approx 2651\,\mathrm{MeV/c^2}$ $N = 40,\quad A = 31/6,\quad \varepsilon = 19/6$
Ω_c	**Ω_c(2770)^0** $0(^3/_2{}^+)$, $Dy(\Omega_c{}^0\gamma)$ $m \approx 2m_p + 6\tfrac{1}{2}\, m'_\mu \approx 2792\,\mathrm{MeV/c^2}$ $N = 44,\quad A = 35/6,\quad \varepsilon = 7/2$
Ξ_c	**Ξ_c(3080), ($m^0 - m^+ = 5.28m_e$)** $^1/_2(?^?)$, $Dy(\Lambda_c{}^+ \overline{K}\pi)$ $m \approx 2m_p + 8\tfrac{1}{2}\, m'_\mu \approx 3074\,\mathrm{MeV/c^2}$ $N = 54$
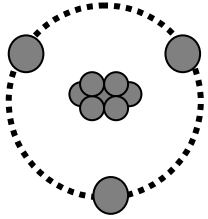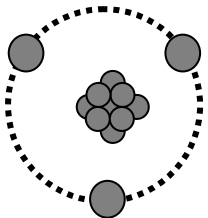
Bottom baryons.   In Tables 3a,b the proposed structures for some bottom baryons are given. The (J = ½) bottom baryon designs are similar to the (J = ½) charmed baryons, with $6m_p$ replacing the $2m_p$ spin-loop. All but one have a lower mass central core of zero spin. A trineon here might have the substance of a proton/anti-proton pair within a radius of $(\pi/2)(e^2/6m_p c^2)$, which is $137(2/\pi)$ times less than the spin-loop radius. The mass range of bottom baryons is small, from ($6m_p$) for $\Lambda_b{}^0$(5619.58) to ($6m_p + 3m'_\mu$) for $\Omega_b{}^-$(6046.1).

Where appropriate, the mass difference between charged components of a baryon is given. For example, in $\Sigma_b^+(5811.3)$ the mass difference $(m^- - m^+)$ is due to two heavy-electrons orbiting around the positive spin-loop; while for $\Xi_b^0(5791.9)$, the mass difference $(m^- - m^0)$ is due to only the second orbiting heavy-electron.

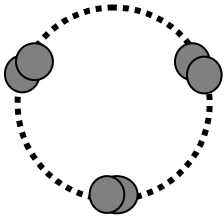Table 3a.   Proposed structure for the lowest bottom baryons with $(J^P = 1/2^+)$.

$\Lambda_b{}^0$	**$\Lambda_b{}^0$ (5619.58)** $0(^1/_2{}^+)$, $\tau = 1.47 \times 10^{-12}$ s, $Dy(\Lambda_c{}^+\ell^-\bar{\upsilon}_\ell)$ $m \approx 6m_p \approx 5629\,MeV/c^2$ $N = 180$
$\Sigma_b{}^+$	**$\Sigma_b{}^+(5811.3)$, $(m^- - m^+ = 8.22m_e)$** $1(^1/_2{}^+)$ $Dy(\Lambda_b{}^0\pi)$ $m \approx 6m_p + 1\tfrac{1}{2}m_\mu{}^/ \approx 5841\,MeV/c^2$ $N = 192$
$\Xi_b{}^0$	**$\Xi_b{}^0(5791.9)$, $(m^- - m^0 = 5.09m_e)$** $^1/_2(^1/_2{}^+)$, $\tau = 1.48 \times 10^{-12}$ s, $m \approx 6m_p + 1\tfrac{1}{2}m_\mu{}^/ \approx 5841\,MeV/c^2$ $N = 191$
$\Omega_b{}^-$	**$\Omega_b{}^-(6046.1)$** $0(^1/_2{}^+)$, $\tau = 1.64 \times 10^{-12}$ s, $Dy(J/\psi\Omega^-)$ $m \approx 6m_p + 3m_\mu{}^/ \approx 6052\,MeV/c^2$ $N = 208$
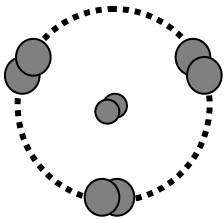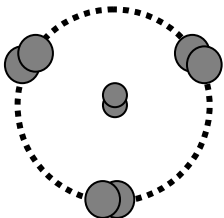
Table 3b.   Proposed structure for the bottom baryons with ($J^P = 3/2^+$).

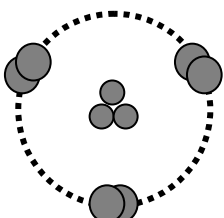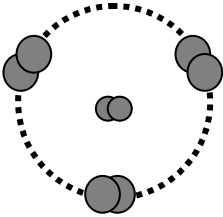| Σ_b | | $\Sigma_b{}^{*+}(5832)$, $(m^- - m^+ = 5.87 m_e)$
 $1(^3/_2{}^+) \, Dy(\Lambda_b{}^0 \pi)$
 $m \approx 6 m_p + 1\tfrac{1}{2} m_\mu' \approx 5841 \, MeV/c^2$
 $N = 193$ |
| Ξ_b | | $\Xi_b(5945)^0$
 $(^3/_2{}^+) \, Dy(\Xi_b{}^- \pi^+)$
 $m \approx 6 m_p + 2\tfrac{1}{2} m_\mu' \approx 5982 \, MeV/c^2$
 $N = 201$ |
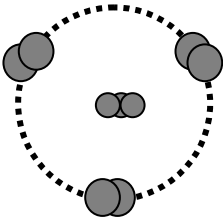
Exotic baryons. In Table 3c the proposed structures for two exotic baryons are given. The designs are similar to the charmed baryons, with $4m_p$ replacing the $2m_p$ spin-loop. They have a lower mass central core of zero spin. Given the decay products, a trineon structure might have the appearance of a pion (ie. matter + anti-matter, see Paper 2) but it is expected to have a radius around $(\pi/2)(e^2/4m_p c^2)$, which is $137(2/\pi)$ times less than the spin-loop radius. Masses are around $(4m_p + 5m_\mu')$, after binding energy losses which depend upon internal orientation detail. These proposed structures are easily accommodated here, between charmed and bottom baryons, without invoking pentaquarks.

Table 3c.   Proposed structure for two exotic baryons.
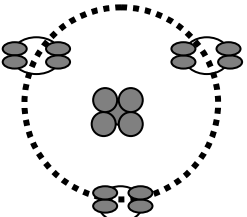
| P_c | | $P_c(4380)^+$
 $(^3/_2{}^?) , \, Dy(J/\psi p)$
 $m \approx 4 m_p + 4\tfrac{1}{2} m_\mu' \approx 4387 \, MeV/c^2$
 $N = 109$ |
| P_c | | $P_c(4450)^+$
 $(^5/_2{}^?) , \, Dy(J/\psi p)$
 $m \approx 4 m_p + 5 m_\mu' \approx 4457 \, MeV/c^2$
 $N = 113$ |
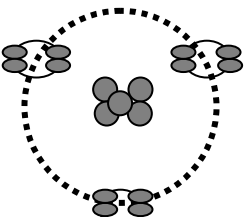
4.   Magnetic moments of baryons.

Proton and neutron magnetic moments were calculated from a simple structural model in Paper 1. Namely, the three positively charged trineons travelled around the proton spin-loop circumference to produce a magnetic moment $2.7928\mu_N$, and in the neutron, one orbiting heavy electron produced a magnetic moment of $-4.70589\mu_N$. Since all baryon designs here are based upon protons, their magnetic moments μ_b probably have similar structural origins and can be interpreted by comparison with the proton.

First, it is only the charge q_s in the positive baryon spin-loop of mass M_1 which produces the actual measured positive magnetic moment:

$$\mu_b = +(q_s \hbar / 2M_1) \quad . \tag{4.1a}$$

We will presume that charge is distributed such that the charge/mass ratio of the spin loop (q_s / M_1) is equal to that observed for the whole baryon (q/M). Then the baryon has a magnetic moment:

$$\mu_b = +(q\hbar / 2M) = +(q/e)(m_p / M)(e\hbar / 2m_p) \quad , \tag{4.1b}$$

where the last factor is the nuclear magneton (μ_N). Therefore, published standardised magnetic moments μ_b must be multiplied by (M/m_p) to reveal the effective charge ratio (q/e) for comparison with the proton (2.7928), see column 3 of Table 4. Thus, only the observed Σ^+ at $(q/e = 3.116)$ can be compared directly with the proton, in order to reveal that its internal mechanism adds 0.116 to the basic value of 3.0, in contrast to the proton wherein 0.207 was subtracted to derive 2.793.

Second, for the neutral baryon, a co-rotating heavy-electron at radius (r_{he}) will produce its own *negative* magnetic moment (μ_{he}):

$$\mu_{he} = -(ecr_{he} / 2) = -(r_{he} / r_p)(e\hbar / 2m_p) = -(r_{he} / r_p)\mu_N \quad , \tag{4.2}$$

where proton spin radius is $[\, r_p = (\hbar / m_p c) = 0.2103 \text{fm} \,]$. This magnetic moment is equal to the difference between the neutral and original positive state, as given in Table 4 by (r_{he} / r_p). Now the heavy-electron mass m_{he} relative to normal electron mass m_e is given by:

$$\frac{m_{he}}{m_e} = \frac{r_{oe}}{r_{he}} = \left(\frac{r_p}{r_{he}}\right) \times \frac{r_{oe}}{r_p} \quad , \tag{4.3}$$

where $(r_{oe} = e^2/m_e c^2 = 2.817940 \text{fm})$ is the classical electron radius. It can be calculated directly, given that r_p and r_{oe} are known, and it should account for the difference (δM) between the original positive baryon mass and the neutral baryon mass. In practice, the measured δM is a little less than the calculated m_{he} because of binding energy loss, see Eq.(10.2.2) of Paper 1.

Table 4   Baryon magnetic moments interpreted in terms of one or two electrons orbiting a proton-type of spin-loop.

	$\mu_b(\mu_N)$	q/e	r_{he}/r_p	m_{he}/m_e	$\delta M/m_e$	χ
p	2.7928	2.7928				
n	-1.913		n - p	n - p	n - p	
			4.706	**2.85**	**2.53**	
(Λ^+)	(2.620)	(3.116)				
Λ^0	-0.613		$\Lambda^0-(\Lambda^+)$	$\Lambda^0-(\Lambda^+)$		
			(3.23)	**(4.11)**		5.5
Σ^+	2.458	3.116				
(Σ^0)	(+0.60)		$\Sigma^0-\Sigma^+$	$\Sigma^0-\Sigma^+$	$\Sigma^0-\Sigma^+$	
			(1.86)	(7.2)	**6.40**	3
Σ^-	-1.160		$\Sigma^--\Sigma^+$	$\Sigma^--\Sigma^+$	$\Sigma^--\Sigma^+$	
			1.25	10.7		1
			2.37	<u>5.65</u>		4
				16.4	**15.8**	
(Ξ^+)	(2.236)	(3.134)				
Ξ^0	-1.250		$\Xi^0-(\Xi^+)$	$\Xi^0-(\Xi^+)$		
			(3.49)	**(3.84)**		6
Ξ^-	-0.651		$\Xi^--(\Xi^+)$	$\Xi^--(\Xi^+)$	$\Xi^--\Xi^0$	
			(1.37)	(9.78)		1.5
			(1.51)	<u>(8.87)</u>		2
				(18.6)	**13.4**	
(Ω^+)	(5.276)	(3.134)				
Ω^-	-2.02		$\Omega^--(\Omega^+)$	$\Omega^--(\Omega^+)$		
			(3.65)	(3.67)		6
			(3.65)	<u>(3.67)</u>		6
				(7.35)		

Notes: Values in round brackets are *estimates* for unmeasured baryons Λ^+, Σ^0, Ξ^+, Ω^+. Column μ_b is the measured moment in nuclear magnetons; **q** is the effective charge in the baryon; r_{he} is the heavy-electron radius around the baryon; ratio r_{he}/r_p is the coefficient of magnetic moment attributable to one or two orbiting heavy-electrons; the heavy-electron mass is given by ($m_{he}/m_e = r_{oe}/r_{he}$); δM is the *measured* increase in baryon mass being attributed to the heavy-electron(s); baryon values of (χ) from Eq.(4.4c) are given. For (Ω^+), the estimated high factor (5.276) is due to its high spin radius for (J = 3/2).

Third, for the negative baryon there are 2 heavy electrons, see $\Sigma^- - \Sigma^+$, with their estimated values of $(r_{he}/r_p)_1 = 1.25$ and $(r_{he}/r_p)_2 = 2.37$, and heavy electron masses which should sum to slightly over the observed result 15.8. This Σ^- had to be allocated two heavy electrons in separate orbits, in order to get viable values for (m_{he}/m_e).

When the baryon cannot be observed directly [as for Λ^+, Σ^0, Ξ^+, Ω^+], its magnetic moment can still be estimated, as shown bracketed in Table 4, so that a viable (m_{he}/m_e) can be postulated. For example, between Ξ^- and Ξ^0 it is $(18.6 - 3.84 = 14.76)$, achieved by proposing $[q/e = 3.134]$ for unobserved (Ξ^+).

It was discovered for the neutron in Paper 1, Eq.(10.2.8), that the relative size of the heavy-electron radius (r_{he}/r_p) satisfies an action integral which serves to stabilise the orbit. The radius of the neutron's heavy-electron $[r_{he} = r_p(e_n\sqrt{3})]$ is critical because quantisation is suggested by the formula:

$$\ln(r_{he}/r_p) \approx \pi/2 \tag{4.4a}$$

This will be interpreted such that the toroidal heavy-electron propagates spiralling circular *feeler* guidewaves inwards from its position at r_{he} to the proton spin-loop at r_p. These are reflected back so continual interaction helps keep the heavy-electron stable in position. For an equivalent guidewave charge δe^2 and mass δm_{he}, the action integral for this loop spiralling inwards and reflecting back is from Eq.(4.4a) by differentiation:

$$2\int_{2\pi r_p}^{2\pi r_{he}} \frac{\delta e^2}{z}dt \approx \int_0^{2\pi} \frac{\delta m_{he}}{2}cr_{he}d\theta \quad , \tag{4.4b}$$

where $(\delta e^2/c = \delta m_{he}cr_{he})$ and $(dz = cdt)$.

Other baryon values of (r_{he}/r_p) can be explained in a similar way to the neutron, such that Eq.(4.4b) should become:

$$2\int_{2\pi r_p}^{2\pi r_{he}} \frac{\delta e^2}{z}dt \approx \chi\int_0^{2\pi} \frac{\delta m_{he}}{2}cr_{he}\left(\frac{1}{e_n^2}\right)d\theta \quad , \tag{4.4c}$$

see values of coefficient χ given in column 7 of Table 4. The $(1/e_n^2)$ term signifies that a third harmonic guidewave is operating, see Eq.(10.3.4) in Paper 1.

The magnetic moment of Σ^+ is anomalously high like the proton in Paper 1 and it may be expressed in a similar way:

$$\mu = (e\hbar / 2M)[3.116 \pm 0.013] \quad ,$$

$$\approx (e\hbar / 2M) \times 3\left\{1 + \frac{1}{(2\pi\alpha^{-1} + 1)}\right\}\left\{1 + \left[\frac{(3m_t / 2)/(3m_e)}{[137(2/\pi)]^2}\right]\left[1 - \left(\frac{(3)24(2/\pi)}{24^2}\right)\right]\right\} \quad . \quad (4.5)$$

$$\underset{\text{3 trineons}}{} \qquad \underset{\text{24 pearls}}{}$$

As for the proton, ($\alpha^{-1} \approx 137$) is the inverse fine structure constant, and there are 24 gluonic-loops constituting a pearl. Each of the three trineons has charge e^+, but unit charge emanates from the spin-loop overall. However, in contrast to the proton, these Σ^+ trineons are aligned *parallel* to their spin-loop and have a weighting factor of $(3m_t / 2)/(3m_e)$, so a higher magnetic moment results for Σ^+. This weighting factor represents the number of charge loops around a trineon in terms of trineon mass ($m_t = m_p / 3$) relative to electron mass per trineon (m_e).

The magnetic moments of (Ξ^+) and (Ω^+) are also anomalous ($q/e = 3.134$), as estimated by setting the trineons and pearls in Eq.(4.5) parallel to the spin-loop, according to Table 1d.

5.   Lifetimes of baryons

Analogous to the neutron in Paper 1, the mean lifetimes of the 4 long-lived baryons might be related to the presence of an orbiting heavy-electron. Given the heavy-electron period ($t_{he} = 2\pi r_{he} / c$), then:

$$t_{he} = (r_{he} / r_p)(2\pi r_p / c) \quad . \quad (5.1)$$

Table 5 lists the (r_{he} / r_p) values from Table 4 and the calculated (t_{he}) values, with the measured lifetimes τ_b. Now if we say ($c\tau_b$) is equal to a number N_b of heavy-electron circumferences (ct_{he}), then upon taking logarithms, we have for Λ^o say in Table 5:

$$\ln(c\tau_b / ct_{he}) \approx 30.54 \approx 137(\pi/2)\,\pi/3e_n{}^2 \quad . \quad (5.2)$$

By differentiating this and introducing ($e^2/c = m_{he}cr_{he}$), an expression for the electromagnetic action around the N_b circumferences is obtained:

$$\int\limits_{(2\pi r_{he}(\pi/2))}^{N_b(2\pi r_{he}(\pi/2))} \frac{e^2}{z'}\,dt \approx 137 \times \int\limits_0^{2\pi} \frac{m_{he}}{2}\,cr_{he}\left(\frac{1}{e_n{}^2}\right)\frac{d\theta}{3} \quad . \quad (5.3)$$

Table 5 Measured baryon lifetimes τ_b relative to the calculated heavy electron periods t_{he}. Baryon Σ^+ has been added because a similar decay law may be operating around its spin-loop.

	r_{he}/r_p	$t_{he}(10^{-23})$ secs	$\tau_b (10^{-10})$ secs	τ_b / t_{he} (10^{13})	$\ln(\tau_b /t_{he})$
n	4.706	2.075	[887.0s]	4.274×10^{12}	59.0172
Λ^o	(3.23)	1.424	2.631	1.847	30.55
Σ^-	2.37	1.053	1.479	1.404	30.27
Ξ^o	(3.49)	1.539	2.90	1.884	30.57
Ξ^-	(1.51)	0.667	1.639	2.458	30.83
Ω^-	(3.65)	1.609	0.822	0.511	29.26
Σ^+		(0.441)	0.8018	(1.82)	(30.53)

Factor e_n^{-2} on the right of this represents third harmonic guidewaves for stabilising the 3 components of the heavy-electron; in agreement with the original neutron equation (10.3.4) in Paper 1. On the left, the unit distance $(2\pi r_{he}(\pi/2))$ is the length of the helix structure around the heavy-electron, rotating at velocity $c' = c(\pi/2)$; see Paper 3, electron model. Length $(z' = c't)$ is then instantaneous length around this helix many times, up to N_b orbits in total. Lifetime distance $c\tau_b$ might represent a coherence length for the guidewaves operating around the heavy-electron, which govern its stability. Table 5 shows that action for the baryons is around half that for the neutron, viz: $\ln(\tau_n /t_{he}) \approx (59.0172)$. For comparison purposes, baryon Σ^+ has been included as it could indicate that a similar decay law is operating around the 3 trineons of its spin-loop.

6.   Compatibility with Standard Model

The model for a static proton in Paper 1 was very successful at explaining the Yukawa potential, the reality of spin and anomalous magnetic moment for structured particles. On the other hand, the QCD Standard Model of particle interactions has been very successful at accounting for observations from high energy collision experiments. The conceptual differences between these two models might be explained if particles in collisions engender characteristics not apparent in static models. That is, the trineons in a proton may interact with incident particles in the same way as quarks do in QCD.

Consider Figure A1 wherein the proton is depicted as trineons A, B, C, travelling around the spin-loop at the velocity of light. Each trineon has a charge (+e) but only emits an electromagnetic field due to (+e/3) into the *exterior* space, so the proton's total external charge is (+e) as observed. Trineons also emit an e.m field in the direction of travel *around* the spin-loop, equivalent to (+2e/3) each.
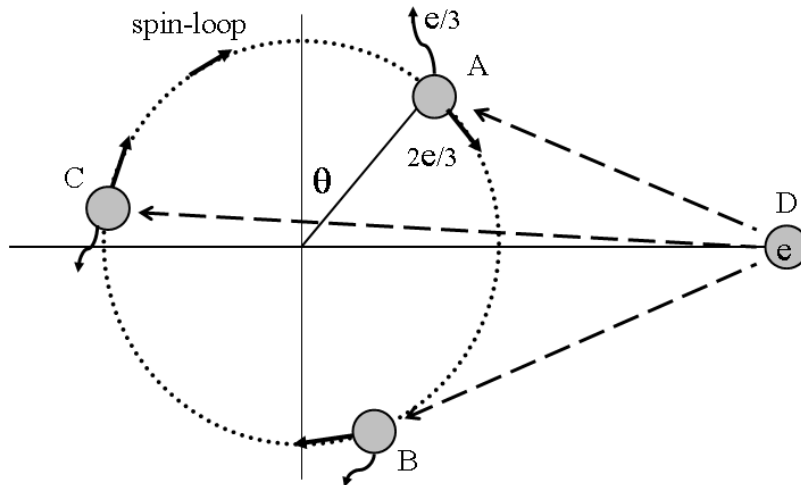

Fig.A1   A schematic proton consisting of 3 trineons in the spin-loop, each with external and internal electromagnetic fields due to charge (e/3) and (2e/3), as experienced by an incident charged particle D.

Consequently, an energetic incident particle D (charge +e) could interact with an individual trineon, depending upon the position and *direction* of that trineon. For example, let interaction of D on A vary as $e[e/3 + (2e/3)\cos(\theta)]$, whereas D on B will vary as $e[e/3 + (2e/3)\cos(\theta+120°)]$, and D on C will vary as $e[e/3 + (2e/3)\cos(\theta+240°)]$. These three interactions of particle D are shown overlaid in Figure A2. Clearly the *effective interaction charge* for each trineon can vary from (e) to (-e/3). The sum for all three trineons is (e).
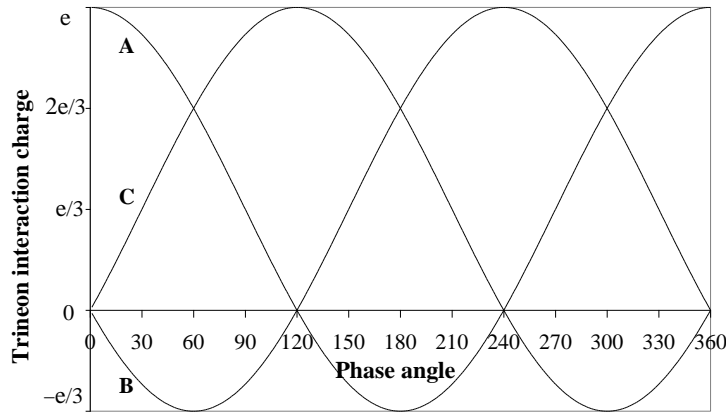
Fig.A2   Variation of *interaction* charge for trineons A,B,C.

For correspondence with the Standard Model, we require the apparent effect of quarks, namely A(+2e/3), B(-e/3), and C(+2e/3), which occur at ($\theta = 60^o$) where the squared values are nearest to each other and sum to (e^2), ie: A($4e^2/9$) + B($e^2/9$) + C($4e^2/9$). The average of $[e/3 + (2e/3)\cos(\theta)]^2$ over one spin-loop cycle, summed for 3 trineons, is also (e^2).

Thus, the effect of a negative *interaction charge* (-e/3) can happen for a collision process wherein a trineon reacts according to its *internal* mechanism and *direction* of travel. Trineons are tightly confined by strong force gluons within a proton, so any collision of an incident particle with a single trineon might appear to involve a quark of spin (1/2).

For the neutron model in Paper 1, a heavy-electron closely orbits the proton to neutralise its *exterior* positive charge. In this case, interaction of D on A varies as e[(2e/3)cos(θ)], whereas D on B will vary as e[(2e/3)cos($\theta+120^o$)], and D on C will vary as e[(2e/3)cos($\theta+240^o$)]. Then the *effective interaction charge* for each trineon can vary from (2e/3) to (-2e/3). The sum for all three trineons is always zero. For correspondence with the Standard Model, we require the apparent effect of quarks such as A(-e/3), B(-e/3), and C(+2e/3), which occurs at ($\theta = 120^o$) where the squared values are nearest to each other.

7.   Conclusions.

Baryon designs in general have been described as being like over developed protons. For many baryons, mass-squared is a function of spin, and quantised action. Empirical magnetic moments have been explained in terms of a positively charged baryon spin-loop surrounded by one or two heavy-electrons. Lifetime of a baryon appears to be related to guidewave coherence around these structures. Within baryon internal structure, conservation

laws are upheld; real spin-radius varies with mass, and mass is understood as localised energy without any ethereal Higgs mechanism. Finally, compatibility with the quarks of the Standard Model has been established regarding interactions between particles.

Acknowledgements

References

Amsler C et al. (2008) Phys Lett B667, 1.

Patrignani C et al. (Particle Data Group), Chin. Phys. C, 40, 100001 (2016) and 2017 update.

Perkins D H (2000) Introduction to High Energy Physics, 4th ed, Cam Univ Press.

Wayte R. (Paper 1) A model of the proton. www.vixra.org/abs/1008.0049.

Wayte R. (Paper 2) A model of mesons. www.vixra.org/abs/1109.0040.

Wayte R. (Paper 3) A model of the electron. www.vixra.org/abs/1007.0055